



Published in final edited form as:

J Mol Biol. 2007 May 25; 369(1): 41–54.

Stable Complexes Formed by HIV-1 Reverse Transcriptase at Distinct Positions on the Primer-Template Controlled by Binding Deoxynucleoside Triphosphates or Foscarnet

Peter R. Meyer^{1,†}, Wiriya Rutvisuttinunt^{1,†}, Suzanne E. Matsuura¹, Antero G. So², and Walter A. Scott^{1,*}

¹Departments of Biochemistry and Molecular Biology, University of Miami Miller School of Medicine, Miami, Florida 33101.

²Department of Medicine, University of Miami Miller School of Medicine, Miami, Florida 33101.

Summary

Binding of the next complementary dNTP by the binary complex containing HIV-1 reverse transcriptase (RT) and primer-template induces conformational changes that have been implicated in catalytic function of RT. We have used DNase I footprinting, gel electrophoretic mobility shift, and exonuclease protection assays to characterize the interactions between HIV-1 RT and chain-terminated primer-template in the absence and presence of various ligands. Distinguishable stable complexes were formed in the presence of foscarnet (an analogue of pyrophosphate), the dNTP complementary to the first (+1) templating nucleotide or the dNTP complementary to the second (+2) templating nucleotide. The position of HIV-1 RT on the primer-template in each of these complexes is different. RT is located upstream in the foscarnet complex, relative to the +1 complex, and downstream in the +2 complex. These results suggest that HIV-1 RT can translocate along the primer-template in the absence of phosphodiester bond formation. The ability to form a specific foscarnet complex might explain the inhibitory properties of this compound. The ability to recognize the second templating nucleotide has implications for nucleotide misincorporation.

Keywords

human immunodeficiency virus; polymerase translocation; DNase I footprinting; exonuclease protection; phosphonofornate

Introduction

Conformational changes are well established during catalytic activity by DNA and RNA polymerases.^{1,2} A rate-limiting conformational change after binding of the complementary incoming dNTP but before phosphodiester bond formation has been proposed on the basis of kinetics experiments.^{3–8} Further evidence for a large conformational change has been provided by numerous experiments showing that a stable complex is formed between polymerase and primer-template (P/T) upon binding of dNTP that dissociates very slowly in the absence of

[†]P.M. and W.R. contributed equally to this work.

*Corresponding author: Mailing address: Department of Biochemistry and Molecular Biology, University of Miami Miller School of Medicine, P.O. Box 016129, Miami, Florida 33101-6129 Phone: (305) 243-6359 Fax: (305) 243-3065 E-mail: wscott@med.miami.edu

Publisher's Disclaimer: This is a PDF file of an unedited manuscript that has been accepted for publication. As a service to our customers we are providing this early version of the manuscript. The manuscript will undergo copyediting, typesetting, and review of the resulting proof before it is published in its final citable form. Please note that during the production process errors may be discovered which could affect the content, and all legal disclaimers that apply to the journal pertain.

phosphodiester bond formation.⁹⁻¹⁶ The occurrence of a major structural rearrangement during catalysis is further supported by comparison of crystal structures of ternary complexes containing a replicative DNA polymerase, chain-terminated P/T, and the incoming dNTP, with binary complexes consisting of only the enzyme and the nucleic acid substrate.¹⁷⁻²³ The polymerase molecule resembles a right hand with a DNA-binding cleft surrounded by subdomains designated as “fingers”, “thumb” and “palm”.²⁴ Upon binding dNTP, rearrangements occur at multiple positions in the enzyme. The largest movements occur in the fingers domain, which rotate through 20° to 60° so that the new base pair is partially enclosed and the complex is converted from an “open” structure to a “closed” one.²⁵ The conformational change has been proposed to contribute to fidelity of dNTP selection, correct positioning of the amino acid side chains responsible for catalysis, and maintenance of processive DNA synthesis.¹ The relationship of the open-to-closed transformation to the general catalytic mechanism for DNA synthesis is uncertain since some X- and Y-family (nonreplicative) polymerases do not undergo this transformation upon binding dNTP^{26,27} and the transformation that occurs in DNA polymerase β is not strictly coupled with catalysis.²⁸⁻³⁰

The replication enzyme for HIV-1, reverse transcriptase (RT), forms a stable complex with chain-terminated P/T and the next complementary dNTP.^{11-14, 31} Comparison of crystal structures of ternary complexes^{20,32} with those of binary complexes^{33,34} show an open-to-closed transformation. Electrophoretic mobility shift experiments with the pyrophosphate (PPi) product analogue, phosphonoformate (fosfarnet), show that a stable complex can also be formed with this compound,³⁵⁻³⁷ suggesting that the enzyme can adopt a closed conformation in the presence of either dNTP substrate or PPi product. Crystal structures of polymerase•P/T•PPi complexes have recently been reported for T7 RNA polymerase,³⁸ the Y-family DNA polymerase Dpo4,³⁹ and the X-family DNA polymerase pol- λ .⁴⁰

The HIV-1 RT•P/T•dNTP ternary complex contains RT in the post-translocational position with the incoming dNTP in position to form a new phosphodiester bond^{20,32} and crystal structures of the HIV-1 RT•P/T binary complex also contain RT in the post-translocational position^{33,34} indicating that the presence of the incoming dNTP is not required for the enzyme to occupy the post-translocational position. Sarafianos et al.⁴¹ obtained crystal structures of RT bound to 3'-azido-3'-deoxythymidine (AZT)-terminated P/T in either the pre- or post-translocational positions by covalently crosslinking RT to the P/T. The pre-translocation structure contained a displaced peptide loop containing the YMDD motif leading these authors to propose a spring-loaded translocational mechanism in which the pre-translocational binary complex is a short-lived intermediate in DNA synthesis and the post-translocational structure is favored under conditions of active nucleotide incorporation. Götte et al.^{37,42,43} determined the position of HIV-1 RT on the P/T using chemical cleavage procedures, which showed that RT could occupy either the pre- or post-translocational position but was shifted to the post-translocational position in response to addition of the next complementary dNTP and to the pre-translocational position in the presence of fosfarnet. In the absence of ligand, the distribution of RT between these two sites was influenced by the incubation temperature and the primer-template sequence.

In the present report we extend the characterization of stable complexes containing RT, P/T and the next complementary dNTP (+1 complex) or fosfarnet (fosfarnet complex). In addition, we show that a stable complex can be formed with dNTP complementary to the +2 position on the template (+2 complex). The +1 complex contains RT in the post-translocation position, as expected. In the fosfarnet complex, the enzyme occupies the pre-translocation position and, in the +2 complex, RT is hypertranslocated and occupies a position downstream from that occupied in the +1 complex.

Results

Effects of the +1 complementary dNTP on deoxyribonuclease I (DNase I) protection and stable complex formation by HIV-1 RT

To probe the interactions between HIV-1 RT and chain-terminated P/T, a DNase I protection assay was employed (Figure 1(a)). [³²P]-ddAMP-terminated L32 primer annealed to WL50 template was incubated in the absence or presence of HIV-1 RT and the indicated concentrations of dTTP, the dNTP complementary to the next nucleotide position on the template, followed by limited digestion with DNase I. Addition of HIV-1 RT, in the absence of dTTP, caused protection from DNase I digestion of a large portion of the primer out to about position -25, except for positions -17, -19 and -20. (The 3'-terminus of the primer and the complementary base on the template are designated as position -1; the first unpaired base on the template is +1.) In the presence of increasing concentrations of dTTP the protection pattern changed. The addition of dTTP induced protection at positions -17 and -20, and hypersensitivity at position -18; while position -19 remained unprotected. Figure 1(b) shows dTTP-dependent induction of stable dead-end complex (DEC) formation using the same chain-terminated P/T. Increasing dTTP concentrations induced stable DEC formation by a larger portion of the P/T, which could be observed as an increase in labeled DNA in the slower migrating position in the electrophoretic mobility shift assay (EMSA). Figure 1(c) shows quantification of the data presented in Figure 1(a) and 1(b).

DNase I protection assays were also used to probe the interactions between RT and the template strand (Figure 1(d)). The addition of dTTP was associated with an increase in overall protection of a large portion of the template with the exception of position -22, which became hypersensitive to DNase I. A quantitative comparison of the dTTP dependence of template hypersensitive site formation, protection at position -7 and DEC formation is shown in Figure 1(e) and a comparison of apparent K_{ds} ($K_{d,app}$ s) for various dTTP-dependent phenomena is shown in Figure 1(f). The dTTP concentrations needed for 50% induction of DEC (1.3 μ M), dTTP-induced protection of primer position -20 (0.68 μ M) and template position -7 (1.3 μ M), and for dTTP-induced DNase I hypersensitivity at primer position -18 (0.60 μ M) and at template position -22 (0.6 μ M) were similar, suggesting that the changes in DNase I protection and hypersensitivity induced by the addition of dTTP and DEC formation are related phenomena.

Effects of non-complementary dNTPs on DNase I protection and stable complex formation by HIV-1 RT

To determine whether the nucleotide-induced changes were dependent on base-pairing with the next nucleotide on the template, DNase I protection (Figure 2(a)) and DEC formation by HIV-1 RT (Figure 2(b)) were studied in the presence of increasing concentrations of each of the non-complementary dNTPs. Only dTTP induced hypersensitivity at position -18 (indicated by the black arrow) suggesting that the -18 hypersensitive site was specific for the complementary dNTP. The protection pattern was similar in the absence of added dNTP or after addition of either dATP or dCTP; however, addition of dGTP induced hypersensitivity to DNase I cleavage of position -17 (indicated by the white arrow), which differed by one base from the position seen with dTTP. In addition, a small amount of stable complex formation was observed by EMSA analysis when high concentrations of dGTP were added (Figure 2(b)). Since the second templating base was dC, we surmised that the effect of dGTP might be caused by an ability of HIV-1 RT to recognize the +2 position of the template and that the addition of the dNTP complementary to this position could induce formation of a stable complex (+2 complex). To determine whether the effect of dGTP was due to its ability to base pair with the +2 position of the template, the DNase I footprints and EMSA experiments were repeated using a P/T with the +2 position on the template changed from C to T. With this P/T there was no

change in the DNase I footprint by addition of dGTP or dCTP; however, addition of dATP caused hypersensitivity at position -17 (Figure 2(c)) and DEC formation (Figure 2(d)). When the +2 position in the template was changed to G, increasing concentrations of dCTP but not of the other noncomplementary dNTPs induced hypersensitivity at position -17 (Figure 2(e)) and DEC formation (Figure 2(f)). These results indicate that HIV-1 RT can recognize the +2 position in the template and the addition of the dNTP complementary to the +2 templating nucleotide can induce formation of a +2 complex. The position of the hypersensitive site in the DNase I protection assays suggests that HIV-1 RT in the +2 complex is primarily located one base downstream compared to its position in the +1 complex.

Effects of foscarnet on DNase I protection and stable complex formation by HIV-1 RT

Figure 3(a) shows that increasing concentrations of foscarnet induced protection at positions -17 and -18 and concomitant increase in DNase I cleavage at positions -19 and -20 (indicated by arrows). The position of the hypersensitive sites in the presence of foscarnet was similar to the predominant species in the absence of foscarnet. Foscarnet also induced formation of stable complex as detected by EMSA (Figure 3(b)) and the foscarnet concentrations needed for changes in the DNase I protection pattern and DEC formation were approximately the same ($K_{d,app}$ about 50 μ M). Figure 3(c) shows a comparison of DNase I protection and hypersensitivity patterns induced by +1 dNTP (dTTP), +2 dNTP (dGTP), and foscarnet on P/T with label in the primer strand. It is clear that each ligand induced a distinguishable pattern of hypersensitive sites: dTTP at positions -18 and -19, dGTP at position -17, and foscarnet at positions -19 and -20. These results suggest that the relative position of HIV-1 RT is different in each complex. In the +2 complex the enzyme is situated downstream relative to the +1 complex by approximately one base, and in the foscarnet complex it is situated upstream of the +1 complex. The figure also shows that the binary complex has DNase I hypersensitive sites primarily at positions -19 and -20, little or no hypersensitivity to cleavage at position -18, and partial protection at position -17. This result suggests the presence of a mixture of binary complexes at different positions on the P/T with the majority of the HIV-1 RT molecules occupying positions similar to those in the foscarnet complex, a minority of the enzyme molecules in the position of the +2 complex, and little, if any, in the position of the +1 complex.

DNase I protection experiments were repeated with P/Ts in which the L32 primer was extended by one nucleotide and terminated with ddTMP, 2',3'-dideoxy-3'-deoxythymidine-5'-monophosphate (d4TMP), or AZTMP (Figure 4) to evaluate complex formation in a different P/T sequence context and with different terminal structures. With the ddTMP-terminated P/T (Figure 4, left panel), RT alone protected a large portion of the primer, with the exception of primer position -18 (solid arrow). With foscarnet, hypersensitivity was observed at primer position -19 (dashed arrow), while in the presence of the +1 dNTP (dGTP), primer position -18 was hypersensitive. These results suggest that, in L33-ddTMP P/T binary complex, RT favored the +1 position in contrast to the results with the L32-ddAMP P/T. Also, in contrast to the ddAMP-terminated P/T, +2 dNTP (dATP) did not induce hypersensitive site formation in the downstream position. For the L33-d4TMP P/T (Figure 4, middle panel), the pattern of protection and hypersensitivity was similar to that of the ddTMP-terminated P/T, with the binary complex favoring the +1 position. However, with the AZTMP-terminated P/T (Figure 4, right panel), the binary complex favored the -1 position, with a strong hypersensitive site at position -19. In summary, the complexes formed between HIV-1 RT and a chain-terminated P/T depended not only on the availability of different binding ligands, but also on the P/T sequence and the nature of the chain-terminator present at the 3'-end of the primer.

Exonuclease mapping of the upstream border of HIV-1 RT bound to chain-terminated P/T

The positions of RT in each of the complexes was further investigated by exonuclease mapping of the barriers to nuclease digestion created by RT bound to P/T in the absence or presence of

foscarnet, +1 dNTP or +2 dNTP. To preserve the integrity of the 3'-terminus of the primer, digestion was performed with 5'-specific exonucleases. For upstream mapping, we used lambda exonuclease, which prefers 5'-phosphorylated ends of double-stranded DNA.⁴⁴ The L32 primer was 5'-phosphorylated, annealed with WL50 template and chain-terminated/3'-labeled by incorporation of [³²P]ddAMP. The P/T was incubated in the absence or presence of HIV-1 RT and the indicated ligand, followed by addition of lambda exonuclease (Figure 5a). In the absence of HIV-1 RT, the majority of the radioactivity was detected in limit digestion products of 10-12 nucleotides. This was also true in the presence of RT alone or in the presence of RT and either dATP or dCTP (non-complementary to both the +1 and +2 positions on the template). In the presence of dGTP, dTTP or foscarnet, distinct barriers to digestion were observed that differed for each of the ligands (see quantitative results, Figure 5b). Mapping of barriers to digestion from the 5' end of the 3'-labeled primer for these three complexes is illustrated in Figure 5c. With dTTP or foscarnet, limit digestion products were almost completely absent, indicating that digestion stopped at the barriers in all or nearly all of the molecules. A major barrier was observed at -29, for dTTP complex, and at -30, for foscarnet complex. This suggests that ternary complexes with these ligands remained stable during the incubation period and that exonuclease was only rarely able to penetrate past the barriers. With dGTP, the barriers were also observed as a cluster of bands corresponding to barriers at positions -26 to -28, but limit digestion products were also observed suggesting that the dGTP complex was less stable. These results suggest that, in agreement with the results of the DNase I protection assays, foscarnet, +1 and +2 dNTPs induced formation of distinct complexes in which the upstream border of the RT molecule was situated in different positions relative to the P/T. RT was primarily located one base upstream in the foscarnet complex and one or more bases downstream in the +2 complex relative to its position in the +1 complex.

Exonuclease mapping of the downstream border of HIV-1 RT bound to chain-terminated P/T

For mapping from the downstream side of RT on the P/T, the single-strand specific 5' exonuclease RecJ_f was used.⁴⁵ The WL65 template was 3'-labeled with [³²P]ddAMP and annealed with L32 primer followed by chain-termination of the primer with unlabeled ddAMP. The P/T was incubated in the absence or presence of HIV-1 RT and the indicated ligand followed by digestion with RecJ_f (Figure 6a). Digestion products were observed in the presence or absence of various ligands. Similar patterns of digestion products were observed with RT alone, and with noncomplementary nucleotides, dATP or dCTP, which was also the pattern seen in the absence of RT. Unique patterns of RecJ_f digestion products were observed with RT and P/T when dGTP, dTTP or foscarnet was added (quantitative data are shown in Figure 6b). Mapping of barriers to digestion from the 5' end of the 3'-labeled template for these three complexes is illustrated in Figure 6c. With dTTP (+1 dNTP), two major products of 41 and 42 nucleotides in length were observed corresponding to barriers to RecJ_f digestion at positions +8 and +9 relative to the end of the primer. With foscarnet, major digestion products corresponded to barriers at +7 and +8, and with dGTP (+2 dNTP) there was a distinct, albeit weak, product corresponding to a barrier at position +10 relative to the end of the primer. The fact that exonuclease mapping from both the upstream and downstream sides of the complex and the DNase I hypersensitive sites showed similar displacement in comparison between the complexes suggests that both borders of the bound RT, as well as a site internal to the complex, had repositioned in response to binding the different ligands, which would be consistent with a lateral displacement of the enzyme without substantial change in the extent of its contact with the P/T.

Discussion

Our results show that at least three stable complexes can be formed by HIV-1 RT on a chain-terminated P/T. Each of the three is resistant to dissociation in the presence of heparin and can be detected by EMSA, DNase I footprinting and by the appearance of barriers to 5' exonuclease digestion on the primer and template strands. These complexes are formed in the presence of different ligands, and RT occupies a different position relative to the primer terminus in each complex. The first complex (+1 complex) is consistent with the "closed" structure described by other investigators^{20,42} containing the +1 dNTP that stabilizes RT in the post-translocational position on the P/T. The second (foscarnet complex) contains a product analogue bound to RT in the pretranslocation position on the P/T and is consistent with previous demonstrations of a stable RT•P/T•foscarnet complex by EMSA^{35,36} and by chemical footprinting.³⁷ This complex may be analogous to product PPi complexes observed by crystallography for T7 RNA polymerase,³⁸ *Sulfolobus solfataricus* translesion DNA polymerase IV (Dpo4),³⁹ and human DNA polymerase λ .⁴⁰ In each of these structures, the polymerase is captured in the pre-translocation position. With T7 RNA polymerase, the PPi complex is in a closed configuration. The other two enzymes do not undergo an open-to-closed transition during catalysis and the relationship between ligand binding and catalytically significant conformational changes is unclear. Foscarnet inhibition of DNA synthesis by HIV-1 RT may be mediated by formation of a stable complex with the enzyme bound in a position that is unable to accept the dNTP substrate.

The third complex we have observed is formed upon incubation with dNTP complementary to the +2 position on the template. RT is located downstream from its position in the +1 complex as shown from the position of the DNase I hypersensitive site and barriers to exonuclease digestion. Specificity for the +2 dNTP was shown by replacing the +2 position on the template with different nucleotides and observing that only the dNTP complementary to the +2 position formed a heparin-resistant complex detected by EMSA and a DNase I hypersensitive site consistent with a hypertranslocated position for RT. Barriers to exonuclease digestion of the +2 complex were heterogeneous, with digestion frequently proceeding to barriers more than one nucleotide beyond the exonuclease stop sites observed with the +1 complex (Figures 5). This may suggest that RT in the presence of +2 dNTP occupies various downstream positions on the P/T or that the position of RT is disturbed during incubation with exonuclease – i.e. lambda exonuclease or RecJ_f might push the bound RT one or two nucleotides beyond the site of initial encounter. The fact that the position of the DNase I hypersensitive site in the +2 complex does not show this heterogeneity argues for the latter explanation.

The +2 complex has precedent with a crystal structure of a Dpo4•P/T•ddGTP complex reported by Ling et al.²⁶, which contains two adjacent template bases in the active site, leaving a gap between the primer terminus and the bound +2 nucleotide. Dpo4 is quite different from RT in structure and function and may have special properties related to its role in DNA repair and lesion bypass; however, the replication polymerase, *E. coli* DNA polymerase (Klenow fragment), has also been shown to specifically recognize the +2 dNTP. Ramanathan et al.⁴⁶ showed that Klenow fragment +1 complex formation was enhanced by the addition of +2 dNTP in the absence nucleotide incorporation due to the depletion of Mg²⁺. Our experiments show that HIV-1 RT can bind +2 dNTP and reposition in the absence of +1 dNTP. We did not determine whether this could also happen in the presence of +1 dNTP. Taken together, these results indicate that dissimilar polymerases have the ability to occupy a hypertranslocated position to accommodate +2 nucleotide binding in the absence of phosphodiester bond formation.

Transient stabilization of polymerase•P/T complexes by dNTP complementary to the +2 position on the template has been previously proposed by Bebenek et al.⁴⁷ to explain the high

frequency of -1 frame-shift mutagenesis that is observed for HIV-1 RT. These authors proposed that transient P/T structures are formed in which the primer is misaligned placing the primer terminus just upstream from the +2 position on the template. Incorporation of one or more nucleotides could occur before the correct alignment was restored resulting in synthesis of a DNA strand containing a one-base deletion. This model is supported by the observation that "hot spots" for frame-shift mutagenesis often follow short homopolymeric runs in the template that could stabilize the transient misaligned structure by allowing an extrahelical nucleotide to find the position that could be most readily accommodated on the enzyme structure.⁴⁷ Even though high concentrations of +2 dNTP were required to obtain detectable levels of +2 complex in our experiments, lower levels of +2 complexes that might be present at physiological dNTP concentrations could have significant implications. A rate of one single-base frameshift mutation per 4,300 nucleotides polymerized has been reported for HIV-1 RT,⁴⁸ corresponding to less than 0.03% of normal nucleotide incorporation events. The +2 complex might account for as much as 0.03% of the population of RT•P/T complexes present at physiological concentrations of dNTPs and could contribute to the high level of frameshift mutagenesis.

A cocrystal structure of human DNA polymerase λ containing misaligned P/T with an extrahelical base has recently been reported.⁴⁰ A similarly misaligned P/T structure has also been proposed for prokaryotic and eukaryotic transcription complexes to explain misincorporation that is dependent on the NTP complementary to the +2 nucleotide on the template.^{49,50} In the case of the transcription complexes, it appears that the P/T realigns after the misincorporation but before further elongation and the resulting mismatched primer terminus is efficiently extended leading to a single base substitution rather than a frame-shift mutation. The ability of RT to accommodate an extrahelical nucleotide is unknown. In our experiments, both the upstream barrier to exonuclease and the hypersensitive site for DNase I cleavage are shifted forward in the presence of the +2 dNTP, suggesting that the complex does not contain an extrahelical nucleotide downstream from the DNase I hypersensitive cleavage site. Our results would be more consistent with a structure like that observed with Dpo4 in which two adjacent template bases occupy the polymerase active site.²⁶ We used the P/Ts shown in Figure 2, but with the ddAMP replaced with dAMP, to test for dNTP specificity in misincorporation assays (data not shown). These experiments failed to show an influence of the +2 template nucleotide on the specificity of dNTP misincorporation arguing against a significant role for the +2 complex in misincorporation in our experiments. However, the studies of Bebenek et al.,⁴⁷ suggest that sequence context is crucial, and the +2 complex may only lead to frame-shift mutagenesis when preceded by specific sequence contexts such as homopolymeric runs that can stabilize a transient structure containing an extrahelical nucleotide.

Most DNase I footprints previously reported for retroviral or retrotransposon RTs⁵¹⁻⁵⁴ were performed in the presence of saturating dNTP concentrations and gave patterns similar to those seen for the +1 complex in our experiments; however, Lavigne et al.⁵⁵ observed hypersensitive sites at the same positions in the presence or absence of the +1 dNTP for most of the P/Ts they tested. In one out of seven P/Ts, appearance of the hypersensitive site was induced by addition of +1 dNTP suggesting that the enzyme usually occupies the +1 or post-translocational position even in the absence of the +1 dNTP. Marchand et al.³⁷ reached a similar conclusion using chemical footprinting methods to determine the position of RT in the binary complex. The P/T used in most of our experiments appears to be one of those rare sequences that favor RT binding in the pre-translocation position since the enzyme shifted forward in the direction of DNA synthesis upon binding +1 dNTP or +2 dNTP, but did not change position when the foscarnet complex was formed (Figures 1(a) and 3(a)). By contrast, the P/T used for the experiment in Figure 4 favored RT binding in the post-translocation position since formation of foscarnet complex shifted the enzyme backward and formation of +1 complex did not change

the position of the hypersensitive site. In addition to sequence context, the position of RT in the binary complex depends on the structure of the chain-terminating residue as shown in Figure 4. The P/T sequence used in that experiment favored the binding of RT in the post-translocational position when terminated with ddTMP or d4TMP but shifted toward the pre-translocation position when terminated with AZTMP. The finding that AZTMP at the primer terminus disfavors occupation of the post-translocation position by RT is consistent with previous reports that +1 dNTP binding is inhibited when the primer terminus is occupied by AZTMP.^{14,42,56-58} Our present results suggest that DNase I hypersensitive site formation, protection from DNase I cleavage, and formation of stable complex by EMSA reflect the same underlying phenomenon, which may correspond to the switch from “open” to “closed” complex configuration and the “locking” of RT to P/T at a specific position determined by ligand binding.

Our results and those of Marchand et al.^{37,42} show that RT can occupy multiple positions on the P/T and that movement between these positions does not depend on nucleotide incorporation. Sarafianos et al.⁴¹ reported the crystal structure of a binary complex with RT in the pre-translocation position in which the YMDD loop was displaced from its expected position. They suggested that this displaced loop could act as a loaded springboard that could provide part of the energy needed to drive translocation of RT to the post-translocation position. These observations support a “power-stroke” mechanism for translocation by comparison with a similar mechanism proposed for translocation by myosin.⁵⁹ A power-stroke mechanism has also been proposed for translocation of T7 RNA polymerase based on comparison of crystal structures of a pretranslocation complex containing product PPi, a post-translocated product complex lacking PPi, and two post-translocation complexes containing the nonhydrolyzable substrate analogue α , β -methylene ATP.^{38,60-62} An alternative mechanism for translocation has been proposed based on experiments with T7 RNA polymerase⁶³⁻⁶⁵ and HIV-1 RT.^{37,42,43} In this mechanism (named the Brownian ratchet mechanism⁶⁶), binary complexes are heterogeneous and can rapidly shift between occupancy of different sites on the P/T. Forward movement of the polymerase is due to binding of the incoming NTP or dNTP, which captures the enzyme in the forward position and allows phosphodiester bond synthesis to occur. Current experimental approaches do not conclusively distinguish between these two mechanisms. The initial translocation event might be masked by rapid repositioning of the enzyme to produce a more stable structure, which could occur too quickly to be detected by available experimental techniques. Nonetheless, we can conclude that repositioning between the +1, +2 and -1 positions is possible in the absence of nucleotide incorporation and that formation and release of PPi would not be necessary to explain translocation.

Experimental Procedures

Expression and purification of poly-histidine tagged HIV-1 RT

Wild-type HIV-1 RT (derived from the BH10 clone of HIV-1)⁶⁷ was expressed in JM109 *Escherichia coli* from an expression vector for wild-type HIV-1 RT containing an N-terminal polyhistidine tag (pHisPKRT) and purified to apparent homogeneity by metal affinity chromatography through His-Bind Resin (Novagen) as previously described.⁶⁸ The specific RNA-dependent DNA polymerase activity of the purified homodimeric enzyme was 20,000 U/mg, where 1U is the amount of enzyme needed for incorporation of 1.0 nmol [³H]-dTTP in 10 min at 37°C using poly(rA)/oligo(dT) as substrate.⁶⁹

Preparation of 3'-³²P-labeled oligonucleotides

To prepare 3'-³²P-labeled L32-ddA/WL50 P/T, 16 pmoles L32 primer (5'-CTACTAGTTTTCTCCATCTAGACGATACCAGA-3') was annealed with excess WL50 template (5'-

GAGTGTGAGGTCTTCATTCTGGTATCGTCTAGATGGAGAAAAGTAG-3') or templates WL50-35T or WL50-35G that differed from WL50 by a single nucleotide substitution 35 bases from the 3' end (see Figure 2) and incubated with 50 μ Ci (10 pmoles) [α -³²P]ddATP and 20 pmoles HIV-1 RT in 300 μ l RB buffer (40 mM Na HEPES, pH 7.5, 20 mM MgCl₂, 60 mM KCl, 1 mM DTT, 2.5 % glycerol, 80 μ g/ml BSA) for 30 min at 37°C. To prepare 3'-labeled L33-dT-analogue terminated P/T, L32 primer annealed to excess WL50 template was labeled and terminated by incubation with 50 μ Ci (10 pmoles) [α -³²P]dATP, 40 μ M ddTTP, d4TTP or AZTTP and 20 pmoles HIV-1 RT in 300 μ l RB buffer for 30 minutes at 37°C. For lambda exonuclease mapping experiments the 5'-end of the L32 primer was phosphorylated by T4 polynucleotide kinase (New England Biolabs) and unlabeled ATP prior to annealing with template and adding the 3' label. Labeled P/Ts were phenol/chloroform and chloroform extracted and ethanol precipitated and resuspended in DNA buffer (10 mM Na HEPES pH 7.4 and 60 mM KCl).

To prepare 3'-³²P-labeled template, 16 pmoles WL50 template was incubated with 20 U terminal deoxynucleotidyl transferase (New England Biolabs) and 20 pmoles [α -³²P]ddATP in 50 μ l NEB buffer 4 (50 mM K acetate, 20 mM Tris-acetate pH 7.9, 10 mM Mg acetate, 1 mM dithiothreitol) containing 0.25 mM CoCl₂ at 37°C for 2 h. The reaction was stopped by heating at 90°C for 10 min, extracted with phenol/chloroform and chloroform, precipitated with ethanol, resuspended in DNA buffer, and annealed with unlabeled L32 primer. The primer was subsequently terminated with ddAMP by adding RT and unlabeled ddATP. For experiments with exonuclease RecJ_f, the template WL65 (5'-GCCTGACCATGTACAGAGTGCTGATCTCCTCATTCTGGTATCGTCTAGATGGAGAA AACTAGTAG-3') was 3'-labeled with [³²P]ddAMP as above prior to annealing with unlabeled L32 primer and termination with RT and unlabeled ddAMP. [α -³²P]dATP was purchased from PerkinElmer Life Sciences. [α -³²P]ddATP and unlabeled NTPs and dNTPs were from Amersham (currently, GE Healthcare). Unlabeled dNTPs were also obtained from Pan Vera Corp. (currently, a part of Invitrogen Corp.) d4TTP was kindly provided by Dr. Raymond F. Schinazi. Selected DNase I footprint analyses with +2 dNTP were repeated with highly purified dNTPs purchased from the alternative sources to test for the possibility that low level contamination of nucleotide stocks might influence the results. No differences dependent on the source of dNTPs were observed. Oligodeoxyribonucleotides were prepared by the DNA core laboratory at the University of Miami, or purchased from Sigma-Genosys.

DNase I protection assay

Five fmoles of labeled P/T was incubated with 200 fmoles RT and the indicated amounts of dNTP in 10 μ l RB buffer for 15 min at 37°C. After incubation on ice for 5 min, 0.03 U DNase I (USB corp.), in RB buffer, was added and the samples were incubated at room temperature for 3 min. The DNase I digestion was stopped by heating at 90°C for 3 minutes followed by addition of 13 μ l loading buffer (16 M urea, 180 mM Tris-HCl, 60 mM taurine, 1 mM EDTA, 0.25% [w/v] bromophenol blue and 0.25% [w/v] xylene cyanol). The samples were reheated for 4 min at 90°C and separated by electrophoresis through a 20% denaturing (8M urea) polyacrylamide gel, at 2000 V for 3-4 h in TTE buffer (90 mM Tris-HCl, 30 mM taurine, 0.5 mM EDTA). The gels were dried and the radioactivity visualized by exposure on X-ray film and quantified by phosphorimaging. The radioactivity in the band of interest (either protected or enhanced) was first normalized to the radioactivity in the band at position -28 (outside of the protected region) to correct for differences in the amount of DNase I used and/or the amount of the sample loaded. The percent of dNTP-induced protection was calculated as $100 - (100 \times B_n/B_0)$ where B_n is the radioactivity in the protected band at the dNTP concentration = n and B_0 is the radioactivity in the band in the absence of dNTP. The resulting values were plotted against dNTP concentration and fitted to a one-ligand binding curve, using SigmaPlot 4.0, to determine the $K_{d,app}$ for the dNTP-induced protection. To calculate the percent dNTP-induced

hypersensitivity, the radioactivity detected in the hypersensitive band in the absence of dNTP was deducted from the radioactivity detected in the presence of various dNTP concentrations and the percent hypersensitivity was determined relative to the maximal amount of radioactivity detected at any dNTP concentration. The data were plotted against dNTP concentration and fitted to a one-ligand binding curve to determine $K_{d,app}$ for the dNTP-induced hypersensitivity.

Electrophoretic mobility shift assay for detection of DEC

Five nM [32 P]ddAMP-terminated P/T was incubated with 200 nM RT and various amounts of dNTP or foscarnet (Sigma-Aldrich), as indicated in the figure legends, in 10 μ l RB buffer for 15 min at 37°C. After incubation on ice for 5 min, 3 μ l heparin/loading dye (0.03 U heparin/ μ l, 30% [v/v] sucrose, 0.25% [w/v] bromphenol blue and 0.25% [w/v] xylene cyanol) in RB buffer was added to dissociate binary complexes. The samples were separated by electrophoresis through an 8% native polyacrylamide gel at 200 V for 1 h at 4°C using Tris-aurine buffer (90 mM Tris, 30 mM taurine). The radioactivity was visualized by exposure on X-ray film and quantified through phosphorimaging. The percentage of band-shifted DNA, after deduction of complex formed in the absence of dNTP, was plotted against the dNTP concentration, and the $K_{d,app}$ for DEC was obtained by fitting the data to a one-ligand binding curve.

Exonuclease protection mapping

For upstream mapping of the borders of the stable complexes, 5 nM 3'-[32 P] ddAMP-terminated, 5'-phosphorylated L32 primer annealed to excess WL50 template was incubated with 200 nM HIV-1 RT and dNTP, foscarnet or no ligand as indicated in the figures, in 10 μ l RB buffer for 15 min at 37°C, followed by incubation at 4°C for 5 min. After addition of 1.2 U lambda exonuclease (USB Corp.), the samples were incubated at 37°C for 8 min followed by heat-inactivation at 90°C for 5 min. For downstream mapping of the borders of the stable complexes, 5 nM 3'-[32 P]ddAMP-labeled WL65 template annealed to excess ddAMP-terminated L32 primer was incubated with 12.5 nM WT HIV-1 RT and ligand (0.8 mM dNTP, 3.2 mM foscarnet, or no ligand) in 10 μ l RB buffer for 15 min at 37°C, followed by incubation at 4°C for 5 min. Ten units of RecJ_f (New England Biolabs) were added and the samples were incubated at 37°C for 10 min followed by heat-inactivation at 90°C for 5 min. For both upstream and downstream mapping, 12 μ l loading buffer were added and the products were separated by electrophoresis through a denaturing 20% polyacrylamide gel.

Acknowledgements

We thank Raymond Schinazi for providing d4TTP and Thomas Kunkel for helpful discussion and insight into the project. This work was supported by NIH grant AI-39973 (to W.A.S), an amfAR postdoctoral fellowship 70567-31-RF (to P.R.M), and an American Heart predoctoral fellowship 0215082B (to W.R).

Abbreviations used

HIV-1, human immunodeficiency virus type 1; RT, reverse transcriptase; P/T, primer-template; PP_i, pyrophosphate; AZT, 3'-azido-3'-deoxythymidine; DNase I, deoxyribonuclease I; DEC, dead-end complex; EMSA, electrophoretic mobility shift assay; $K_{d,app}$, apparent K_d ; d4T, 2',3'-didehydro-3'-deoxythymidine.

References

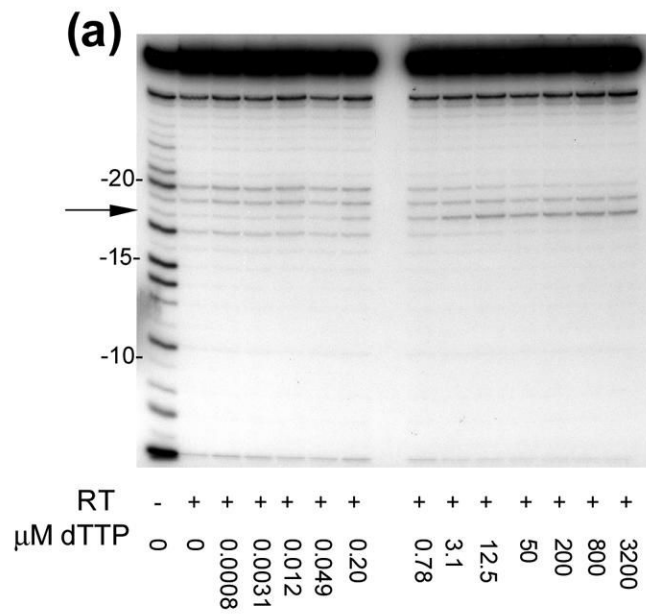
1. Johnson KA. Conformational coupling in DNA polymerase fidelity. *Annu. Rev. Biochem* 1993;62:685–713. [PubMed: 7688945]
2. Landick R. Active-site dynamics in RNA polymerases. *Cell* 2004;116:351–353. [PubMed: 15016367]

3. Mizrahi V, Henrie RN, Marlier JF, Johnson KA, Benkovic SJ. Rate-limiting steps in the DNA polymerase I reaction pathway. *Biochemistry* 1985;24:4010–4018. [PubMed: 3902078]
4. Kuchta RD, Mizrahi V, Benkovic PA, Johnson KA, Benkovic SJ. Kinetic mechanism of DNA polymerase I (Klenow). *Biochemistry* 1987;26:8410–8417. [PubMed: 3327522]
5. Patel SS, Wong I, Johnson KA. Pre-steady-state kinetic analysis of processive DNA replication including complete characterization of an exonuclease-deficient mutant. *Biochemistry* 1991;30:511–525. [PubMed: 1846298]
6. Dahlberg ME, Benkovic SJ. Kinetic mechanism of DNA polymerase I (Klenow fragment): identification of a second conformational change and evaluation of the internal equilibrium constant. *Biochemistry* 1991;30:4835–4843. [PubMed: 1645180]
7. Kati WM, Johnson KA, Jerva LF, Anderson KS. Mechanism and fidelity of HIV reverse transcriptase. *J. Biol. Chem* 1992;267:25988–25997. [PubMed: 1281479]
8. Frey MW, Sowers LC, Millar DP, Benkovic SJ. The nucleotide analog 2-aminopurine as a spectroscopic probe of nucleotide incorporation by the Klenow fragment of *Escherichia coli* polymerase I and bacteriophage T4 DNA polymerase. *Biochemistry* 1995;34:9185–9192. [PubMed: 7619819]
9. Fisher PA, Korn D. Ordered sequential mechanism of substrate recognition and binding by KB cell DNA polymerase α . *Biochemistry* 1981;20:4560–4569. [PubMed: 7295634]
10. Reardon JE, Spector T. Herpes simplex virus type 1 DNA polymerase. Mechanism of inhibition by acyclovir triphosphate. *J. Biol. Chem* 1989;264:7405–7411. [PubMed: 2540193]
11. Müller B, Restle T, Reinstein J, Goody RS. Interaction of fluorescently labeled dideoxynucleotides with HIV-1 reverse transcriptase. *Biochemistry* 1991;30:3709–3715. [PubMed: 1707667]
12. Spence RA, Kati WM, Anderson KS, Johnson KA. Mechanism of inhibition of HIV-1 reverse transcriptase by nonnucleoside inhibitors. *Science* 1995;267:988–993. [PubMed: 7532321]
13. Rittinger K, Divita G, Goody RS. Human immunodeficiency virus reverse transcriptase substrate-induced conformational changes and the mechanism of inhibition by nonnucleoside inhibitors. *Proc. Natl. Acad. Sci. USA* 1995;92:8046–8049. [PubMed: 7544013]
14. Tong W, Lu C-D, Sharma SK, Matsuura S, So AG, Scott WA. Nucleotide-induced stable complex formation by HIV-1 reverse transcriptase. *Biochemistry* 1997;36:5749–5757. [PubMed: 9153415]
15. Dzantiev L, Romano LJ. A conformational change in *E. coli* DNA polymerase I (Klenow fragment) is induced in the presence of a dNTP complementary to the template base in the active site. *Biochemistry* 2000;39:356–361. [PubMed: 10630996]
16. Gangurde R, Modak MJ. Participation of active-site carboxylates of *Escherichia coli* DNA polymerase I (Klenow fragment) in the formation of a prepolymerase ternary complex. *Biochemistry* 2002;41:14552–14559. [PubMed: 12463755]
17. Pelletier H, Sawaya MR, Kumar A, Wilson SH, Kraut J. Structures of ternary complexes of rat DNA polymerase β , a DNA template-primer, and ddCTP. *Science* 1994;264:1891–1903. [PubMed: 7516580]
18. Sawaya MR, Prasad R, Wilson SH, Kraut J, Pelletier H. Crystal structures of human DNA polymerase β complexed with gapped and nicked DNA: evidence for an induced fit mechanism. *Biochemistry* 1997;36:11205–11215. [PubMed: 9287163]
19. Doublé S, Tabor S, Long AM, Richardson CC, Ellenberger T. Crystal structure of a bacteriophage T7 DNA replication complex at 2.2 Å resolution. *Nature* 1998;391:251–258. [PubMed: 9440688]
20. Huang H, Chopra R, Verdine GL, Harrison SC. Structure of a covalently trapped catalytic complex of HIV-1 reverse transcriptase: implications for drug resistance. *Science* 1998;282:1669–1675. [PubMed: 9831551]
21. Li Y, Korolev S, Waksman G. Crystal structures of open and closed forms of binary and ternary complexes of the large fragment of *Thermus aquaticus* DNA polymerase I: structural basis for nucleotide incorporation. *EMBO J* 1998;17:7514–7525. [PubMed: 9857206]
22. Franklin MC, Wang J, Steitz TA. Structure of the replicating complex of a pol α family DNA polymerase. *Cell* 2001;105:657–667. [PubMed: 11389835]
23. Johnson SJ, Taylor JS, Beese LS. Processive DNA synthesis observed in a polymerase crystal suggests a mechanism for the prevention of frameshift mutations. *Proc. Natl. Acad. Sci. USA* 2003;100:3895–3900. [PubMed: 12649320]

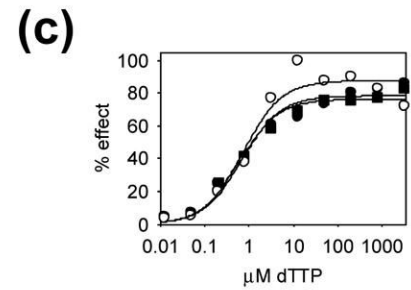
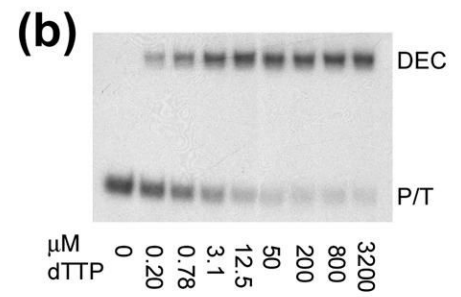
24. Ollis DL, Brick P, Hamlin R, Xuong NG, Steitz TA. Structure of large fragment of *Escherichia coli* DNA polymerase I complexed with dTMP. *Nature* 1985;313:762–766. [PubMed: 3883192]
25. Kunkel TA, Bebenek K. DNA replication fidelity. *Annu. Rev. Biochem* 2000;69:497–529. [PubMed: 10966467]
26. Ling H, Boudsocq F, Woodgate R, Yang W. Crystal structure of a Y-family DNA polymerase in action: a mechanism for error-prone and lesion-bypass replication. *Cell* 2001;107:91–102. [PubMed: 11595188]
27. Garcia-Diaz M, Bebenek K, Krahn JM, Kunkel TA, Pedersen LC. A closed conformation for the Pol λ catalytic cycle. *Nat. Struct. Mol. Biol* 2005;12:97–98. [PubMed: 15608652]
28. Arndt JW, Gong W, Zhong X, Showalter AK, Liu J, Dunlap CA, Lin Z, Paxson C, Tsai M-D, Chan MK. Insight into the catalytic mechanism of DNA polymerase β : structures of intermediate complexes. *Biochemistry* 2001;40:5368–5375. [PubMed: 11330999]
29. Vande Berg BJ, Beard WA, Wilson SH. DNA structure and aspartate 276 influence nucleotide binding to human DNA polymerase β . Implication for the identity of the rate-limiting conformational change. *J. Biol. Chem* 2001;276:3408–3416. [PubMed: 11024043]
30. Showalter AK, Tsai M-D. A reexamination of the nucleotide incorporation fidelity of DNA polymerases. *Biochemistry* 2002;41:10571–10576. [PubMed: 12186540]
31. Sharma B, Kaushik N, Singh K, Kumar S, Pandey VN. Substitution of conserved hydrophobic residues in motifs B and C of HIV-1 RT alters the geometry of its catalytic pocket. *Biochemistry* 2002;41:15685–15697. [PubMed: 12501197]
32. Tuske S, Sarafianos SG, Clark AD Jr, Ding J, Naeger LK, White KL, Miller MD, Gibbs CS, Boyer PL, Clark P, Wang G, Gaffney BL, Jones RA, Jerina DM, Hughes SH, Arnold E. Structures of HIV-1 RT-DNA complexes before and after incorporation of the anti-AIDS drug tenofovir. *Nat. Struct. Mol. Biol* 2004;11:469–474. [PubMed: 15107837]
33. Jacobo-Molina A, Ding J, Nanni RG, Clark AD Jr, Lu X, Tantillo C, Williams RL, Kamer G, Ferris AL, Clark P, Hizi A, Hughes SH, Arnold E. Crystal structure of human immunodeficiency virus type 1 reverse transcriptase complexed with double-stranded DNA at 3.0 Å resolution shows bent DNA. *Proc. Natl. Acad. Sci. USA* 1993;90:6320–6324. [PubMed: 7687065]
34. Ding J, Das K, Hsiou Y, Sarafianos SG, Clark AD Jr, Jacobo-Molina A, Tantillo C, Hughes SH, Arnold E. Structure and functional implications of the polymerase active site region in a complex of HIV-1 RT with a double-stranded DNA template-primer and an antibody Fab fragment at 2.8 Å resolution. *J. Mol. Biol* 1998;284:1095–1111. [PubMed: 9837729]
35. Meyer PR, Matsuura SE, Zonarich D, Chopra RR, Pendarvis E, Bazmi HZ, Mellors JW, Scott WA. Relationship between 3'-azido-3'-deoxythymidine resistance and primer unblocking activity in foscarnet-resistant mutants of human immunodeficiency virus type 1 reverse transcriptase. *J. Virol* 2003;77:6127–6137. [PubMed: 12743270]
36. Cruchaga C, Ansó E, Rouzaut A, Martínez-Irujo JJ. Selective excision of chain-terminating nucleotides by HIV-1 reverse transcriptase with phosphonoformate as substrate. *J. Biol. Chem* 2006;281:27744–27752. [PubMed: 16829515]
37. Marchand B, Tchesnokov EP, Götte M. The pyrophosphate analogue foscarnet traps the pre-translocational state of HIV-1 reverse transcriptase in a Brownian ratchet model of polymerase translocation. *J. Biol. Chem* 2007;282:3337–3346. [PubMed: 17145704]
38. Yin YW, Steitz TA. The structural mechanism of translocation and helicase activity in T7 RNA polymerase. *Cell* 2004;116:393–404. [PubMed: 15016374]
39. Vaisman A, Ling H, Woodgate R, Yang W. Fidelity of Dpo4: effect of metal ions, nucleotide selection and pyrophosphorolysis. *EMBO J* 2005;24:2957–2967. [PubMed: 16107880]
40. Garcia-Diaz M, Bebenek K, Krahn JM, Pedersen LC, Kunkel TA. Structural analysis of strand misalignment during DNA synthesis by a human DNA polymerase. *Cell* 2006;124:331–342. [PubMed: 16439207]
41. Sarafianos SG, Clark AD Jr, Das K, Tuske S, Birktoft JJ, Ilankumaran P, Ramesha AR, Sayer JM, Jerina DM, Boyer PL, Hughes SH, Arnold E. Structures of HIV-1 reverse transcriptase with pre- and post-translocation AZTMP-terminated DNA. *EMBO J* 2002;21:6614–6624. [PubMed: 12456667]

42. Marchand B, Götte M. Site-specific footprinting reveals differences in the translocation status of HIV-1 reverse transcriptase. Implications for polymerase translocation and drug resistance. *J. Biol. Chem* 2003;278:35362–35372. [PubMed: 12819205]
43. Götte M. Effects of nucleotides and nucleotide analogue inhibitors of HIV-1 reverse transcriptase in a ratchet model of polymerase translocation. *Curr. Pharm. Des* 2006;12:1867–1877. [PubMed: 16724953]
44. Little JW. Lambda exonuclease. *Gene Amplif. Anal* 1981;2:135–145. [PubMed: 6242844]
45. Lovett ST, Kolodner RD. Identification and purification of a single-stranded-DNA-specific exonuclease encoded by the *recJ* gene of *Escherichia coli*. *Proc. Natl. Acad. Sci. USA* 1989;86:2627–2631. [PubMed: 2649886]
46. Ramanathan S, Chary KVR, Rao BJ. Incoming nucleotide binds to Klenow ternary complex leading to stable physical sequestration of preceding dNTP on DNA. *Nucl. Acids Res* 2001;29:2097–2105. [PubMed: 11353079]
47. Bebenek K, Abbotts J, Wilson SH, Kunkel TA. Error-prone polymerization by HIV-1 reverse transcriptase. Contribution of template-primer misalignment, miscoding, and termination probability to mutational hot spots. *J. Biol. Chem* 1993;268:10324–10334. [PubMed: 7683675]
48. Bebenek K, Abbotts J, Roberts JD, Wilson SH, Kunkel TA. Specificity and mechanism of error-prone replication by human immunodeficiency virus-1 reverse transcriptase. *J. Biol. Chem* 1989;264:16948–16956. [PubMed: 2476448]
49. Pomerantz RT, Temiakov D, Anikin M, Vassilyev DG, McAllister WT. A mechanism of nucleotide misincorporation during transcription due to template-strand misalignment. *Mol. Cell* 2006;24:245–255. [PubMed: 17052458]
50. Kashkina E, Anikin M, Brueckner F, Pomerantz RT, McAllister WT, Cramer P, Temiakov D. Template misalignment in multisubunit RNA polymerases and transcription fidelity. *Mol. Cell* 2006;24:257–266. [PubMed: 17052459]
51. Wöhrl BM, Georgiadis MM, Telesnitsky A, Hendrickson WA, Le Grice SFJ. Footprint analysis of replicating murine leukemia virus reverse transcriptase. *Science* 1995;267:96–99. [PubMed: 7528942]
52. Wöhrl BM, Tantillo C, Arnold E, Le Grice SFJ. An expanded model of replicating human immunodeficiency virus reverse transcriptase. *Biochemistry* 1995;34:5343–5350. [PubMed: 7537089]
53. Ghosh M, Howard KJ, Cameron CE, Benkovic SJ, Hughes SH, Le Grice SFJ. Truncating α -helix E' of p66 human immunodeficiency virus reverse transcriptase modulates RNase H function and impairs DNA strand transfer. *J. Biol. Chem* 1995;270:7068–7076. [PubMed: 7535765]
54. Rausch JW, Arts EJ, Wöhrl BM, Le Grice SFJ. Involvement of C-terminal structural elements of equine infectious anemia virus reverse transcriptase in DNA polymerase and ribonuclease H activities. *J. Mol. Biol* 1996;257:500–511. [PubMed: 8648620]
55. Lavigne M, Polomack L, Buc H. Structures of complexes formed by HIV-1 reverse transcriptase at a termination site of DNA synthesis. *J. Biol. Chem* 2001;276:31439–31448. [PubMed: 11402037]
56. Meyer PR, Matsuura SE, Mian AM, So AG, Scott WA. A mechanism of AZT resistance: an increase in nucleotide-dependent primer unblocking by mutant HIV-1 reverse transcriptase. *Mol. Cell* 1999;4:35–43. [PubMed: 10445025]
57. Meyer PR, Matsuura SE, Schinazi RF, So AG, Scott WA. Differential removal of thymidine nucleotide analogues from blocked DNA chains by human immunodeficiency virus reverse transcriptase in the presence of physiological concentrations of 2'-deoxynucleoside triphosphates. *Antimicrob. Agents Chemother* 2000;44:3465–3472. [PubMed: 11083661]
58. Boyer PL, Sarafianos SG, Arnold E, Hughes SH. Selective excision of AZTMP by drug-resistant human immunodeficiency virus reverse transcriptase. *J. Virol* 2001;75:4832–4842. [PubMed: 11312355]
59. Jiang MY, Sheetz MP. Mechanics of myosin motor: force and step size. *Bioessays* 1994;16:531–532. [PubMed: 8085999]
60. Yin YW, Steitz TA. Structural basis for the transition from initiation to elongation transcription in T7 RNA polymerase. *Science* 2002;298:1387–1395. [PubMed: 12242451]

61. Temiakov D, Patlan V, Anikin M, McAllister WT, Yokoyama S, Vassilyev DG. Structural basis for substrate selection by T7 RNA polymerase. *Cell* 2004;116:381–391. [PubMed: 15016373]
62. Steitz TA. Visualizing polynucleotide polymerase machines at work. *EMBO J* 2006;25:3458–3468. [PubMed: 16900098]
63. Guajardo R, Sousa R. A model for the mechanism of polymerase translocation. *J. Mol. Biol* 1997;265:8–19. [PubMed: 8995520]
64. Gelles J, Landick R. RNA polymerase as a molecular motor. *Cell* 1998;93:13–16. [PubMed: 9546386]
65. Guo Q, Sousa R. Translocation by T7 RNA polymerase: a sensitively poised Brownian ratchet. *J. Mol. Biol* 2006;358:241–254. [PubMed: 16516229]
66. Schafer DA, Gelles J, Sheetz MP, Landick R. Transcription by single molecules of RNA polymerase observed by light microscopy. *Nature* 1991;352:444–448. [PubMed: 1861724]
67. D'Aquila RT, Summers WC. HIV-1 reverse transcriptase/ribonuclease H: high level expression in *Escherichia coli* from a plasmid constructed using the polymerase chain reaction. *J. Acquir. Immune Defic. Syndr* 1989;2:579–587. [PubMed: 2479733]
68. Meyer PR, Matsuura SE, So AG, Scott WA. Unblocking of chain-terminated primer by HIV-1 reverse transcriptase through a nucleotide-dependent mechanism. *Proc. Natl. Acad. Sci. USA* 1998;95:13471–13476. [PubMed: 9811824]
69. Tan C-K, Zhang J, Li Z-Y, Tarpley WG, Downey KM, So AG. Functional characterization of RNA-dependent DNA polymerase and RNase H activities of a recombinant HIV reverse transcriptase. *Biochemistry* 1991;30:2651–2655. [PubMed: 1705816]



WL50 3'-.....GGTCTT^ACTTCTG...-5'
 L32-ddA 5'-.....CCAGAA_H



- = DEC formation
- = DNase-1 protection (-20)
- = DNase-1 hypersensitivity (-18)

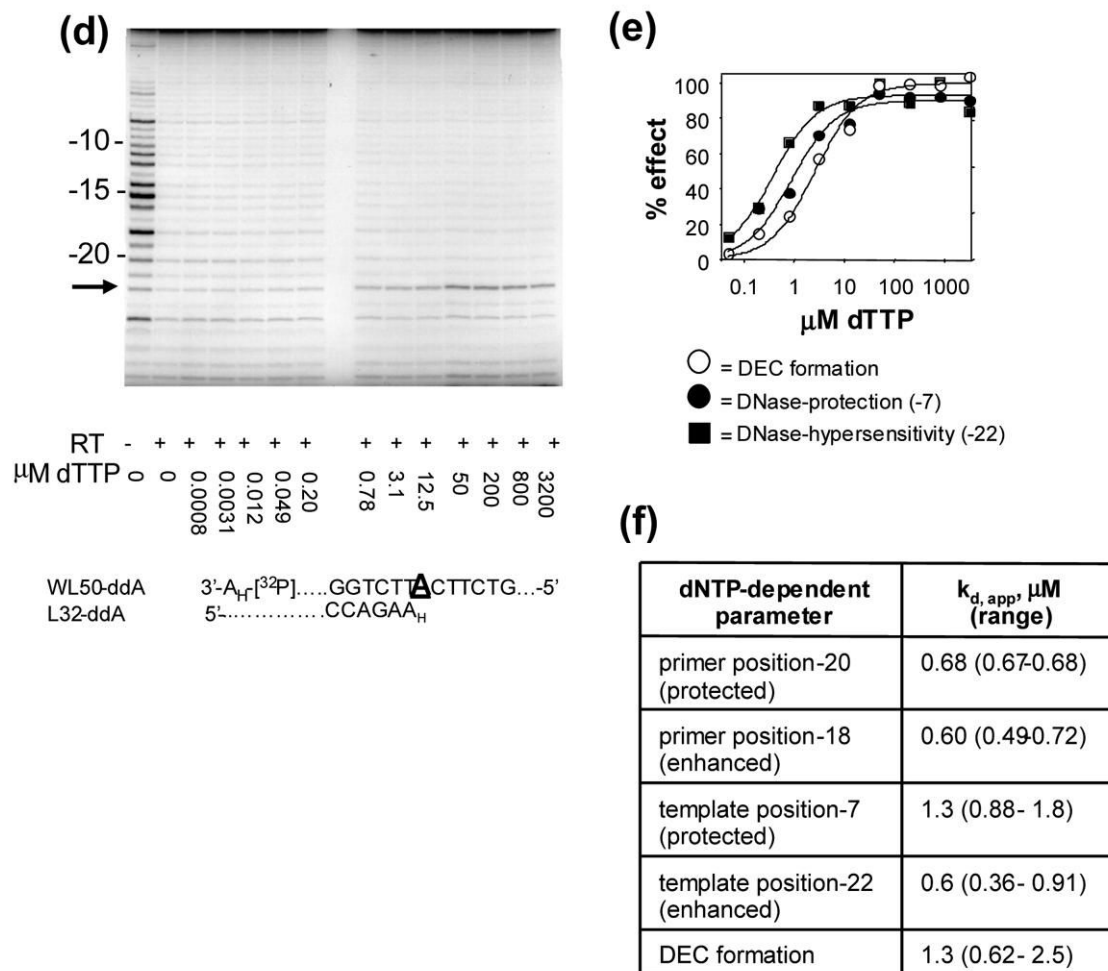


Figure 1. Effects of the next complementary dNTP on DNase I protection and stable complex formation by HIV-1 RT

(a) DNase I footprinting on the 3'-labeled primer strand. Five nM 3'-[³²P]ddAMP-terminated L32 primer annealed to WL50 template was incubated in the absence or presence of 200 nM HIV-1 RT and the indicated concentrations of dTTP followed by 3 min exposure to DNase I. Products were separated by electrophoresis through a 20% denaturing polyacrylamide gel. Numbers to the left of the lanes indicate the positions of the bands. The 3'-terminal nucleotide on the primer is defined as position -1 in this and subsequent figures. The arrow indicates the position of the hypersensitive site induced by dTTP binding formed by cleavage between position -18 and -19 on the primer. A partial sequence of the P/T is shown. The +1 base on the template is bold and underlined. A_H indicates ddA. (b) EMSA detection of stable complex formation. Labeled P/T was incubated with HIV-1 RT as described in (a) in the absence of dTTP or with the indicated concentrations of dTTP. Incubation at 37°C was followed by addition of heparin/loading dye and separation of DEC from free P/T by electrophoresis through an 8% non-denaturing polyacrylamide gel. (c) Quantitative comparison of primer DNase I footprinting and stable complex data as a function of dTTP concentration. The radioactivity in bands at -20 (protected) and -18 (hypersensitive) in (a) and DEC formation in (b) were quantified by phosphorimaging, plotted versus dTTP concentration, and fitted to single-ligand binding curves (solid lines). (d) DNase I footprinting on the 3'-labeled template strand. DNase I footprinting was performed as in (a) but with 3'-[³²P]ddAMP-labeled WL50 template annealed with unlabeled ddAMP-terminated L32 primer. The arrow indicates the

position of the hypersensitive site induced by dTTP binding formed by cleavage between position -21 and -22 on the template. A partial sequence of the P/T is shown. The +1 base on the template is bold and underlined. A_H indicates ddA. (e) Quantitative comparison of template DNase 1 footprinting and stable complex data. The radioactivity in the bands at -7 (protected) and -22 (hypersensitive) in (d) were quantified by phosphorimaging, plotted versus dTTP concentration, and fitted to single-ligand binding curves (solid lines). DEC formation with labeled template is also shown. (f) $K_{d,app}$'s calculated from data from experiments such as those in (c) and (e). The mean and range are shown for at least two experiments for each value.

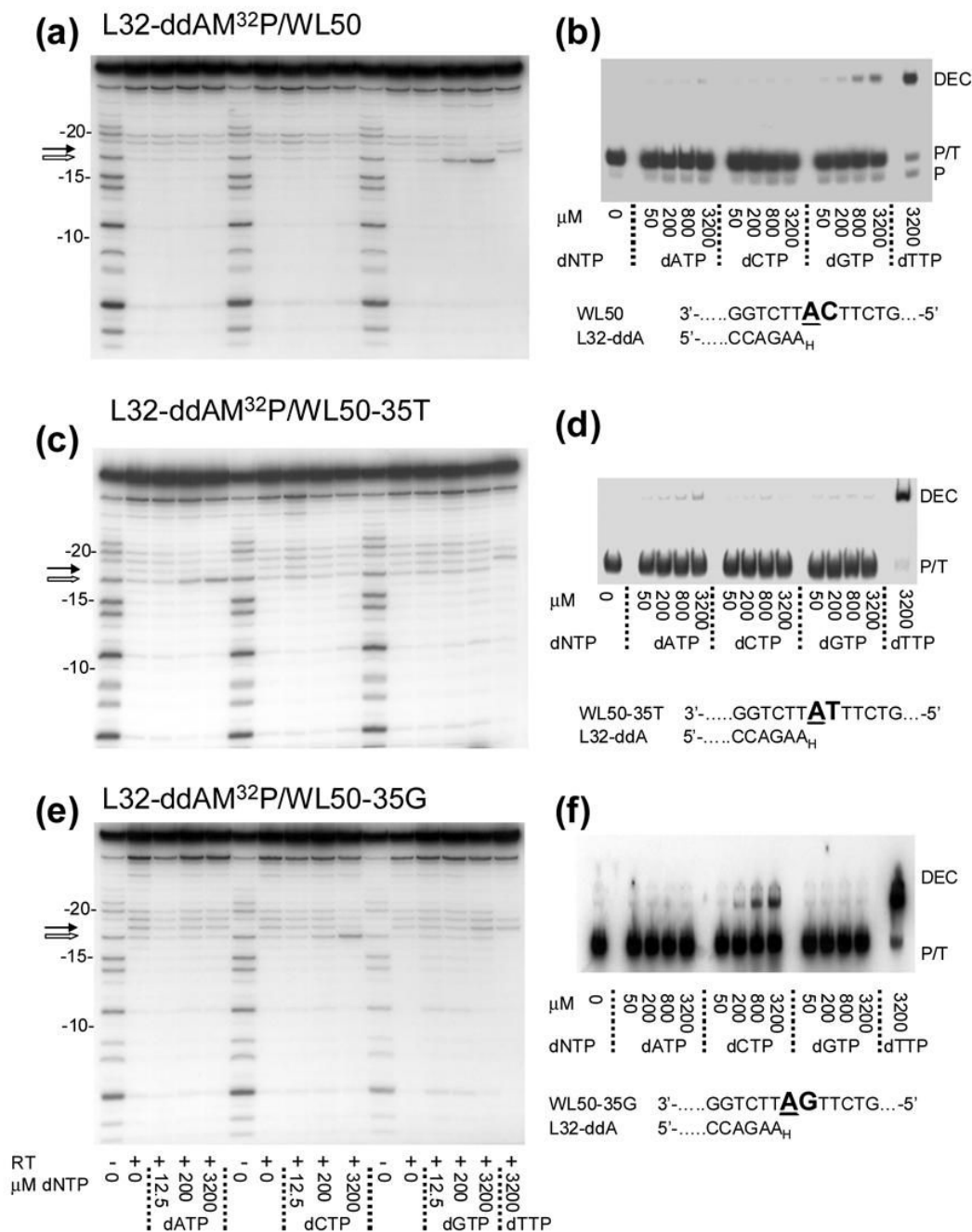


Figure 2. Effects of noncomplementary dNTPs on DNase I footprints and stable complex formation by HIV-1 RT

(a), (c), (e) Five nM 3'-[³²P] ddAMP-terminated L32 primer annealed to the indicated template was incubated in the absence or presence of HIV-1 RT and the indicated concentrations of dATP, dCTP, dGTP or dTTP followed by exposure to DNase I and electrophoresis performed as in Figure 1(a). Band positions are indicated as in Figure 1. The black and white arrows indicate the hypersensitive sites observed for +1 and +2 complexes, respectively. (b), (d), (f) EMSA detection of stable complex formation. Labeled P/Ts were incubated with HIV-1 RT as in (a),(c), and (e), and the concentrations of dNTPs indicated at the bottom of each panel followed by separation of P/T and DEC as described in Figure 1(b). A partial sequence of each

P/T is shown in panels (b), (d) and (f) with the +1 and +2 template nucleotides shown in bold. The +1 nucleotide is underlined. A_H indicates ddA .

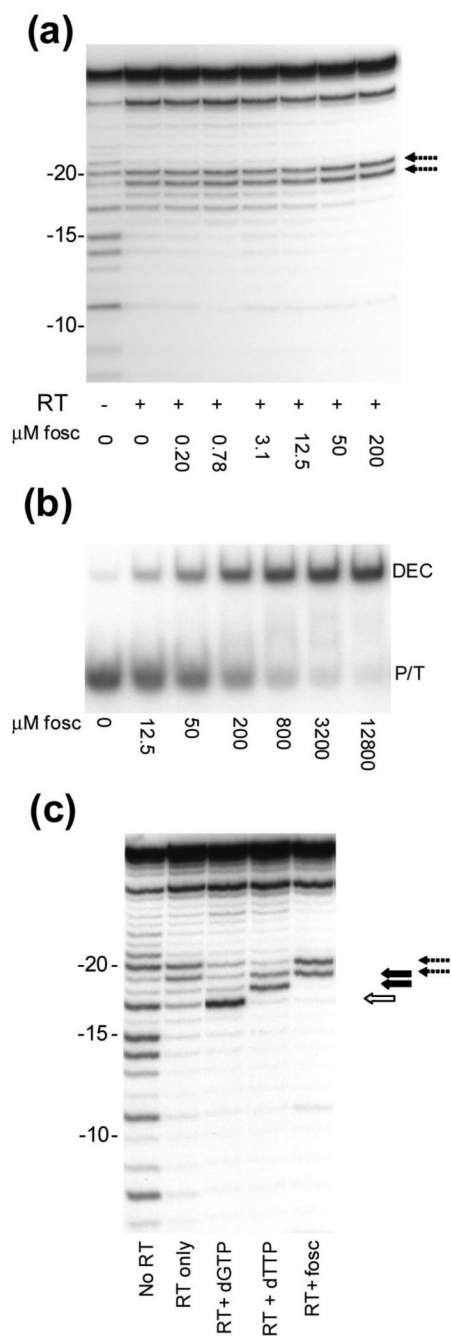


Figure 3. Effects of foscarnet on DNase I protection and stable complex formation by HIV-1 RT
 (a) DNase I footprinting as a function of added foscarnet. Labeled 3'-[³²P]ddAMP-L32/WL50 P/T was incubated in the absence or presence of HIV-1 RT and the indicated concentrations of foscarnet (fosc) followed by exposure to DNase I and electrophoresis performed as in Figure 1(a). Band positions relative to the primer terminus are shown on the left. The arrows indicate the hypersensitive sites induced by foscarnet. (b) EMSA detection of stable complex formation as a function of foscarnet concentration. Labeled P/T was incubated with HIV-1 RT and the indicated concentrations of foscarnet followed by separation of P/T and DEC as described in the legend to Figure 1(b). (c) Comparison of DNase I footprints with 3'-labeled primer with 800 μM dGTP, 800 μM dTTP or 3.2 mM foscarnet. Labeled P/T was incubated in the absence

or presence of HIV-1 RT with the indicated ligand followed by exposure to DNase I and electrophoresis performed as in Figure 1(a). Arrows indicate hypersensitive sites induced by foscarnet (dashed), dTTP (solid black), or dGTP (white).

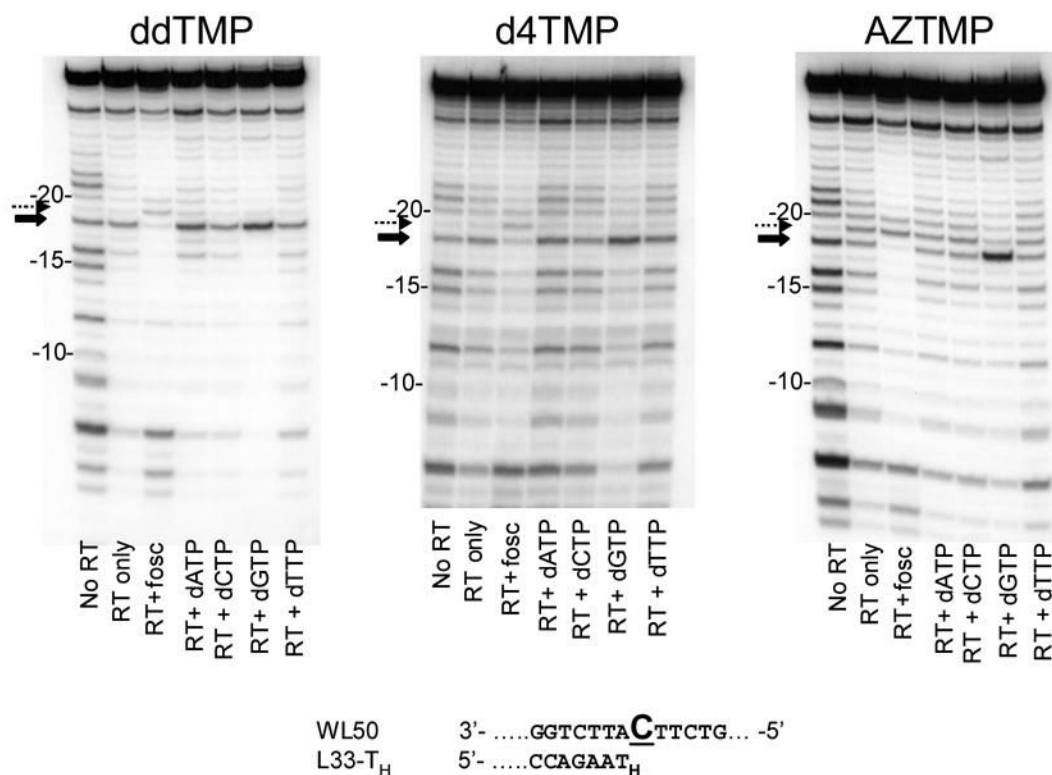


Figure 4. DNase I protection on P/Ts terminated with dT analogues

Five nM L32 primer annealed to WL50 template was extended with [³²P]-dATP, terminated with the indicated dT-analogue and incubated in the absence or presence of 200 nM HIV-1 RT and no ligand, 3.2 mM foscarnet or 200 μM of the indicated dNTP followed by exposure to DNase I and electrophoresis performed as described in Figure 1(a). Band position relative to the primer terminus is indicated to the left of the lanes. The arrows indicate hypersensitive sites induced by foscarnet (dashed) or +1 dNTP (solid). A partial sequence of the P/T is shown where the first downstream templating base is in bold and underlined. T_H indicates the chain-terminating dT-analogue residue in each of the primers (identified at the top of each panel).

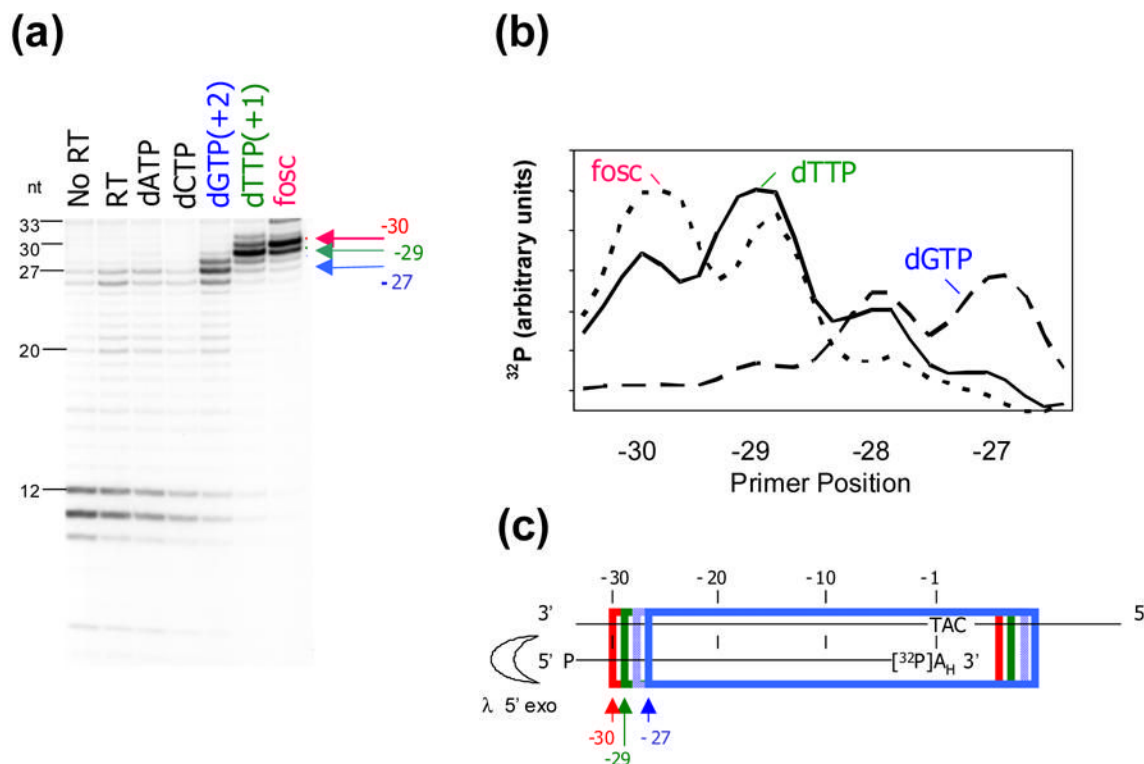


Figure 5. Lambda exonuclease mapping of the upstream borders of HIV-1 RT bound to P/T
 (a) Five nM 5'-phosphorylated, 3'-[^{32}P]ddAMP-labeled L32 primer annealed to WL50 template was incubated in the absence or presence of excess HIV-1 RT and the indicated ligand followed by incubation with lambda exonuclease. Products were separated by electrophoresis through a non-denaturing 20% polyacrylamide gel and the radioactivity visualized through phosphorimaging. The numbers to the left of the lanes indicate the size of the digestion products (in nucleotides). These values also correspond to positions relative to the primer terminus (e.g., 10 indicates the product of digestion that stopped at the bond upstream of position -10, etc.) Arrows on the right of (a) and at the bottom of panel (c) indicate the predominant stop site for lambda exonuclease digestion in the foscarnet complex (red), +1 complex (green) or +2 complex (blue). (b) The radioactivity was quantified using phosphorimaging for digestion products obtained in the presence of foscarnet (short dashes), dTTP (solid line) or dGTP (long dashes) and plotted versus primer position. (c) Diagram showing map positions for predominant barriers to digestion initiated at the phosphorylated 5' end of the 3'-labeled primer by lambda exonuclease (shown by the Pac-Man figure). Overlapping colored rectangles represent expected exonuclease protected regions for each complex. The light blue line corresponds to a weaker barrier at position -28 encountered by lambda exonuclease digestion in the presence of dGTP. Nucleotide positions relative to the primer terminus are shown in the scale at the top of the diagram.

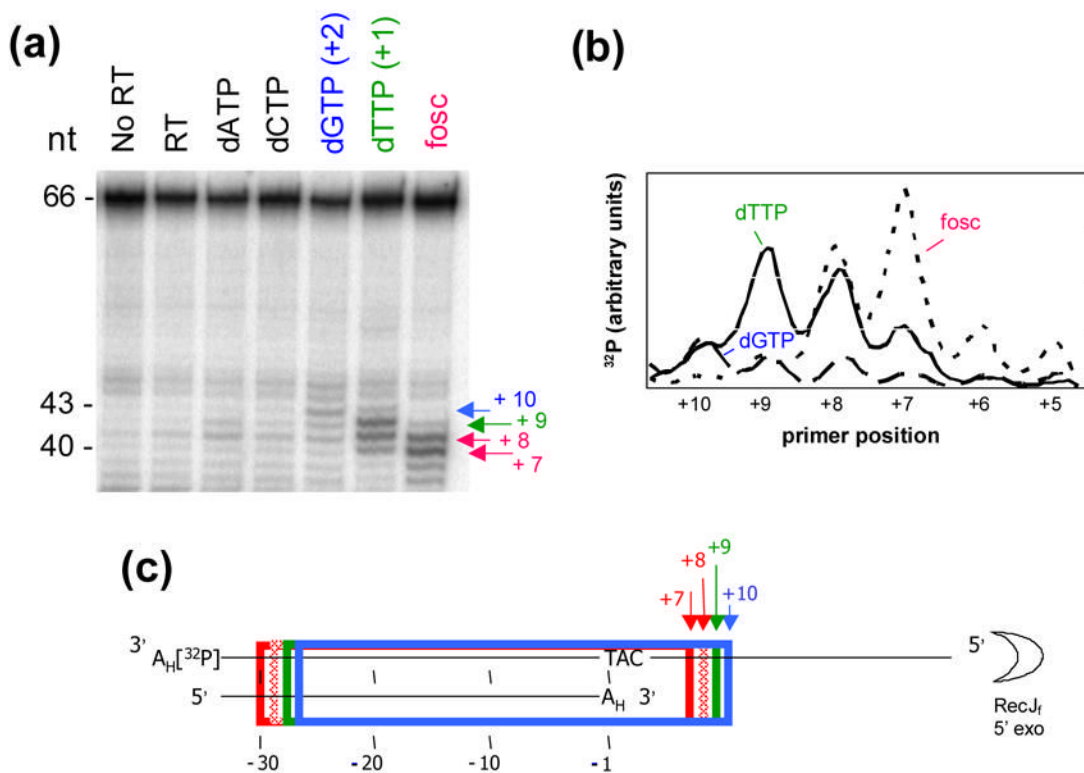


Figure 6. RecJ_f exonuclease mapping of the downstream borders of HIV-1 RT bound to chain-terminated P/T

(a) Five nM 3'-[³²P]ddAMP-labeled WL65 template annealed to unlabeled ddAMP-terminated L32 primer was incubated in the absence or presence of 12.5 nM HIV-1 RT and the indicated ligand (0.8 mM dNTP, 3.2 mM foscarnet or no ligand), followed by incubation with RecJ_f exonuclease as described under Experimental Procedures and electrophoresis performed as in Figure 5. Numbers on the left of the lanes indicate the size of the digestion products (in nucleotides) and the numbers to the right of the lanes indicate the map positions of the predominant downstream barriers to digestion (+1 is the first template base following the primer terminus). The arrows in (a) and (c) indicate predominant barriers to RecJ_f exonuclease digestion (color-coded as in Figure 5). (b) The radioactivity in the gel in (a) was quantified using phosphorimaging for the products of digestion of complexes formed with foscarnet (short dashes), dTTP (solid line) or dGTP (long dashes) and plotted versus distance from the primer terminus. (c) Diagram showing map positions for predominant barriers to digestion initiated at the 5' end of the 3'-labeled template by RecJ_f exonuclease (shown by the Pac-Man figure). Overlapping rectangles represent regions of the P/T protected from exonuclease digestion for each complex. The dark and light red lines correspond to barriers (positions +7 and +8, respectively) encountered by RecJ_f digestion in the presence of foscarnet. Nucleotide positions relative to the primer terminus are shown in the scale at the bottom of the diagram.